Bose-Einstein condensation in atomic hydrogen

T. J. Greytak [1], D. Kleppner, D. G. Fried, T. C. Killian [2], L. Willmann, D. Landhuis, S. C. Moss

Physics Department and Center for Materials Science and Engineering, Massachusetts Institute of Technology, Cambridge, MA 02139, USA

Abstract

The addition of atomic hydrogen to the set of gases in which Bose-Einstein condensation can be observed expands the range of parameters over which this remarkable phenomenon can be studied. Hydrogen, with the lowest atomic mass, has the highest transition temperature, 50 μK in our experiments. The very weak interaction between the atoms results in a high ratio of the condensate to normal gas densities, even at modest condensate fractions. Using cryogenic rather than laser precooling generates large condensates. Finally, two-photon spectroscopy is introduced as a versatile probe of the phase transition: condensation in real space is manifested by the appearance of a high density component in the gas, condensation in momentum space is readily apparent in the momentum distribution, and the phase transition line can be delineated by following the evolution of the density of the normal component.

Keywords: spin-polarized hydrogen; Bose-Einstein condensation; two-photon spectroscopy; cold collision frequency shift

1. Introduction

When our MIT group began studying spin-polarized atomic hydrogen in 1976 it was thought to be the only gas in which there was even a remote chance of obtaining Bose-Einstein condensation. Using a quantum theory of corresponding states Hecht [1] had argued in 1959 that, due to its very light mass and weak interactions, spin-polarized atomic hydrogen would remain a gas down to absolute zero. Interest in hydrogen was revived in 1976 with the publication of many-body calculations [2] confirming that the ground state of spin-polarized atomic hydrogen was indeed a gas. It was also noted that even if there were a way to keep other elements in the gaseous state, hydrogen, being the lightest, would have the highest transition temperature at a given atomic density.

Spin-polarized hydrogen was first stabilized by Silvera and Walraven [3] in 1980 at Amsterdam. In subsequent years groups at British Columbia, Cornell, Harvard, Moscow, and Turku, as well as our own, used spin-polarized atomic hydrogen to study many interesting physical phenomena from collision processes to spin-waves [4]. The observation of BEC remained a long range and elusive goal.

When BEC in a gas was finally observed in 1995 it was in alkali-metal vapors [5–7]. The reasoning

[1] Corresponding author. E-mail: greytak@mit.edu

[2] Present address: Physics Laboratory, National Institute of Standards and Technology, Gaithersburg, MD 20899-8424

Article published in Physica B 280 (2000) 20-26

of 1976, although true, proved to be irrelevant. The ground state of the alkali-metals is certainly a solid. Yet the density in the alkali experiments was so low that the three-body collisions leading to nucleation did not seriously limit the lifetime of the gas. At a gas density of 10^{14} atoms/cm^3 the transition temperature in sodium is 1.5 μK, 23 times lower than it would be in atomic hydrogen. However, the development of laser cooling of atoms allowed the alkali vapors to be pre-cooled to temperatures low enough that evaporative cooling could be used to take them into the sub-μK realm.

Since 1995, many fruitful experiments have been performed using alkali gases, greatly expanding the field of BEC physics. The study of Bose-condensed hydrogen may lead to unique contributions. Hydrogen possesses special attractions in that it affords relatively weak interactions between atoms, the possibility of condensing large numbers of atoms for long periods of time, and atomic states whose energies can be calculated with exquisite accuracy.

2. Trapping and Cooling

The hyperfine diagram of the $1S$ state of atomic hydrogen is shown in Fig. 1. The lowest two states, **a** and **b**, are high field seeking states. They can not be confined in a static magnetic trap because it is not possible to have a maximum in the magnitude of the magnetic field in a source free region. Most of the early experiments on spin-polarized hydrogen were carried out on these states confined by a combination of magnetic fields and liquid helium covered walls. Ultimately, however, recombination into molecules — due to adsorption on the walls at low temperatures or three-body recombination in the gas at high densities — precluded achieving conditions necessary for BEC. Attention then turned to confining the low field seeking states, **c** and **d**, in pure magnetic traps having a local minimum in the field. (Recently Safonov et al. [8] used changes in the surface three-body recombination rate to detect the formation of a quasicondensate

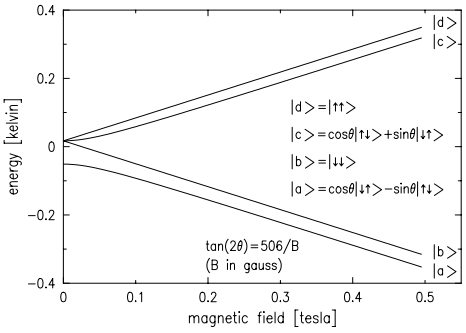

Fig. 1. Hyperfine diagram for the ground state of atomic hydrogen.

in a two-dimensional layer of **b** state atoms.)

The experiments described here were carried out on the doubly polarized **d** state confined in a trap of the Ioffe-Pritchard form. Near the bottom of such a trap the potential rises parabolically from a finite minimum (a bias field is necessary to prevent the spin of the atom from flipping when passing through a zero in the field); thus surfaces of constant magnetic field are ellipsoids of revolution about the vertical axis. A unique feature of our trap is its high aspect ratio of 400:1, the ratio of the major (vertical) axis to the minor axis. The loading of the trap from a low temperature atomic discharge source is described elsewhere [9]. Immediately after loading, the trap contains about 10^{14} atoms at a temperature of 40 mK.

The subsequent cooling of the atoms by three orders of magnitude is carried out by evaporation [10]. The most energetic atoms are allowed to escape from the trap at a rate slow enough that the remaining atoms can continuously readjust their energy distribution to lower temperatures through collisions. A competing mechanism causes heating by removing some of the least energetic atoms from the high density region at the bottom of the trap by two-body spin relaxation. The temperature is determined by a balance between these two mechanisms and comes to steady state at a fraction of the trap depth varying from 1/12 at 40 mK to about 1/7 at 40 μK.

Initially we allow the atoms to escape by lowering the confining potential at one end of the trap

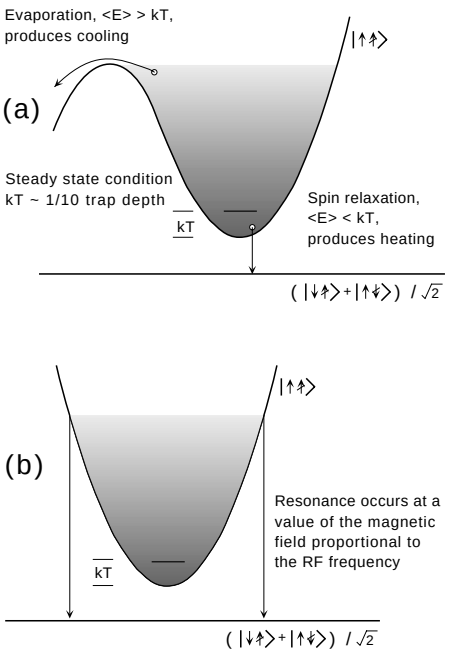

Fig. 2. Sketches of potential energy versus position demonstrating evaporative cooling of hydrogen by (a) lowering a trapping field, or (b) by RF ejection of atoms.

as shown in Fig. 2a. This method becomes inefficient below about 100 μK when atoms promoted to high energy states near the center of the trap have a high probability of losing that energy in a collision before being able to reach the end of the trap and escape [11]. To solve this problem we use RF ejection of the atoms [12] below a temperature of 120 μK. RF ejection was first applied to the evaporative cooling of alkali-metal vapors [13]. An RF magnetic field flips the spins of atoms in that region of the trap having a particular value of the trapping magnetic field (see Fig. 2b). Atoms whose spins are reversed are no longer confined. By starting with an RF field resonant with the highest fields in the trap, then slowly lowering the frequency, successively lower energy atoms can be expelled. Since all the atoms on a specific energy surface in the trap are affected, the process is more efficient than evaporation through one end, particularly in a trap as long and thin as ours. It was the application of RF ejection to the hydrogen that finally allowed us to achieve the conditions necessary for BEC.

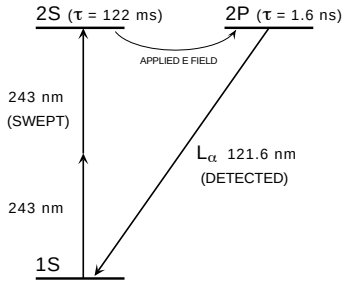

Fig. 3. Two-photon spectroscopy of the $1S$-$2S$ transition in hydrogen.

We monitor the temperature by three different techniques: measuring the shape of the energy distribution as the atoms are rapidly dumped from the trap [14], using the known relation between the temperature and the trap depth, and (at low densities) measuring the time of flight broadening of the Doppler-free part of the two-photon spectrum [15]. The density is determined by measuring the two-body dipole decay rate. The densities quoted in this paper are the maximum densities, those at the bottom of the trap.

3. Two-photon Spectroscopy

We use two-photon spectroscopy of the $1S$-$2S$ transition to study the trapped hydrogen atoms [15]. When illuminated with photons of energy exactly half the $1S$ to $2S$ level spacing, the atoms are promoted to the $2S$ state by the absorption of two photons (see Fig. 3). This differs from the one photon processes used to manipulate and study the alkali-metals in two important ways. First, the resonance is extremely narrow allowing it to be used for very high resolution spectroscopy. Second, the absorption is so weak that we can not detect the resonance by a decrease in the amplitude of the transmitted beam. Instead, we apply an electric field to the atoms which mixes the long lived $2S$ state with the short lived $2P$ state. The atom then returns to the ground state by the emission of a Lyman-α photon. We detect the resonance by recording the Lyman-α production as a function of the frequency of the illuminating beam.

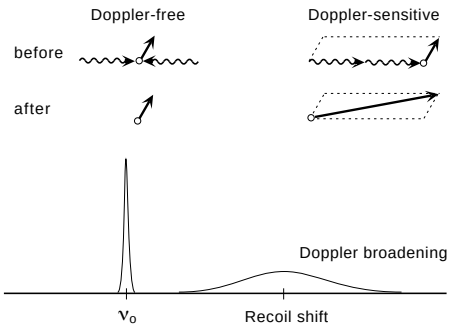

Fig. 4. Features of the two-photon spectrum in a standing wave. For hydrogen the recoil shift referenced to the 243 nm excitation radiation is 6.7 MHz. The Doppler width in this schematic would be appropriate to a temperature of about 50 μK, but the Doppler-free line would be much taller and narrower than indicated.

In our experiment a laser beam at 243 nm is reflected back on itself by a mirror at the bottom of the cell creating a standing wave in the trap. Atoms that absorb two co-propagating photons produce a recoil shifted and Doppler broadened feature in the spectrum (see Fig. 4). The shape of the Doppler line gives the momentum distribution in the gas and thus provides another measure of the temperature. Atoms that absorb two counter-propagating photons transfer no momentum to the atoms. The width of the resulting feature in the spectrum could, in principle, be determined only by the natural lifetime of the $2S$ state. In our experiments, however, the width of this feature is limited to 1 kHz (or one part in 10^{12}) by the finite coherence time of our laser source.

In 1996 Jamieson, Dalgarno and Doyle [16] pointed out that the interactions between the atoms cause a density dependent mean field shift of each of the hydrogen energy levels. They calculated that the resulting shift in the $1S$-$2S$ transition frequency would be negative, proportional to the density, and of a magnitude which would be observable in our experiments. We measured the shift [17] by studying the Doppler-free component in normal hydrogen and found $\Delta\nu_{1S-2S} = 2\Delta\nu_{243nm} = \chi n$, where n is the atomic density and $\chi = -3.8 \pm 0.8 \times 10^{-16}$ MHz cm^3. Since there is a distribution of densities in the trap, the Doppler-free component is broadened as well as shifted by the interaction. The Doppler-sensitive component is broadened and shifted by similar amounts, but these effects are small compared to the Doppler broadening and recoil shift.

4. Bose-Einstein Condensation

Two-photon spectroscopy allowed us to identify three characteristic features of Bose-Einstein condensation: condensation in real space, condensation in momentum space, and the phase diagram [18].

If a non-interacting Bose gas were to be cooled below the transition temperature, a finite fraction of the atoms would fall into the lowest energy single particle quantum state. For a harmonic trap such as that used here, the lowest energy eigenstate is that of a three dimensional harmonic oscillator. This gives rise to a condensation in real space since the spatial extent of the ground state wavefunction is much smaller that that of the normal gas. Consequently the density of atoms would become extremely high over a narrow region at the bottom of the trap. This effect is evident in Fig. 5 which shows the Doppler-free portion of the two-photon spectrum of a gas cooled just below its transition at a temperature of 50 μK and a density of 2×10^{14} cm^{-3}. The strong sharp peak on the right is due to the non-condensed (normal) component and is shifted to the red of the free atom resonance by an amount determined by its density. The weak broad feature, which appears only below the transition, is due to the condensate. Note that a red shift of 0.8 MHz corresponds to a density of 4×10^{15} cm^{-3}, 20 times higher than the density of the normal gas.

The total number of atoms represented in Fig. 5 is 2×10^{10}, determined from the density and the known effective volume of the trap. The fraction of the atoms in the condensate can be determined by examining the ratio of the areas under the condensate and normal features of the spectrum, taking into account the fact that the laser beam illumi-

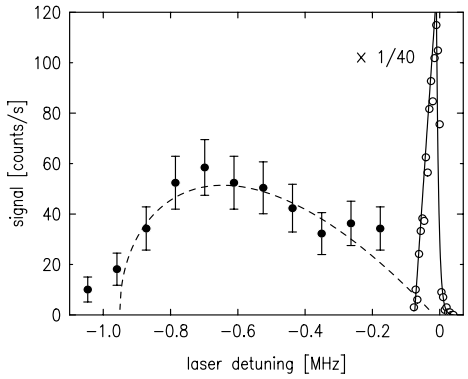

Fig. 5. Doppler-free spectrum of the condensate (broad feature) and the normal component (narrow feature).

nates all of the condensate but only a fraction of the normal gas. We estimate the condensate fraction to be about 5%, corresponding to a total of 10^9 condensate atoms.

If 10^9 atoms were to be put in the single particle ground state of this particular trap, the condensate density would be about 200 times greater than the measured value. The observed density is the result of a mean field repulsion or spreading pressure due to the interactions between the atoms. Since the condensate density is substantially higher than that of the coexisting normal gas, we can treat the condensate using a zero-temperature Thomas-Fermi approximation (a mean field model which neglects the kinetic energy terms). The dashed curve in Fig. 5 shows the Thomas-Fermi density profile for an interacting gas in a parabolic trap with a maximum condensate density of 4.8×10^{15} cm^{-3}. The resulting condensate is 15 μm in diameter and 5 mm in length. This should be compared with the 3 μm diameter which would result from the single particle ground state if there were no interactions. As a self-consistency check one can calculate the condensate fraction from the Thomas-Fermi model using as input parameters the s-wave scattering length, $a_{1S-1S} = 0.0648$ nm [19], the measured maximum condensate density, the temperature of the normal component, and the trap geometry. The calculated condensate fraction is 6%, in good agreement with the value determined by spectral weights [20].

Atom	m (amu)	T_c (μK)	a (nm)	a/λ_T	N_c
H	1	50	0.06	2.7 $\times 10^{-4}$	10^9
Li	7	0.3	-1.5	-1.2 $\times 10^{-3}$	10^3
Na	23	2.0	2.8	1.1 $\times 10^{-2}$	10^7
Rb	87	0.7	5.4	2.4 $\times 10^{-2}$	10^6

Table 1
Typical values of mass, transition temperature, scattering length, perturbation parameter and number of atoms in the condensate for the atomic species that have been Bose condensed.

A quantitative measure of the interactions in low temperature gases is the ratio of the scattering length to the deBroglie wavelength, a/λ_T. As shown in Table 1 this ratio is substantially smaller in hydrogen than in the other BEC gases. It is the weakness of the interactions in hydrogen which allows the ratio of the condensate density to the normal density to be very large, even at modest condensate fractions. Note that the density ratio of 24:1 for the data in Fig. 5 would, for a homogeneous gas, only be reached at a reduced temperature $T/T_c = 0.12$. Thus for many purposes our condensates are nearly pure and can be treated by zero-temperature models.

Textbook treatments of Bose-Einstein condensation in a homogeneous gas emphasize condensation in momentum space. A drastic reduction in momentum also occurs for condensate atoms in a trap since the momentum spread is determined only by the uncertainty principle and the spatial extent of the condensate. Therefore a very narrow feature should appear in the Doppler-sensitive portion of the two-photon spectrum accompanying the formation of the condensate. In our case, where the condensate has a length of about 5 mm along the propagation direction of the photons, the Doppler width would be about 100 Hz. Note that this is narrower than would be the case for non-interacting atoms in the single particle ground state. Although this intrinsic width is obscured in our experiments by the distribution of density shifts in the condensate, the resulting width is still much narrower than the Doppler width of the normal component. (Stenger et al. [21] have recently

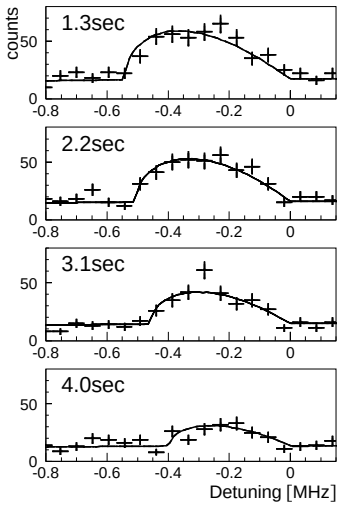

Fig. 6. Condensate feature sitting on top of the much broader contribution from the normal component in the Doppler-sensitive portion of the two-photon spectrum. Times are measured from the end of forced evaporative cooling. The number of atoms in the condensate is about the same as in Fig. 5, but the trap volume is larger resulting in a lower condensate density.

used two-photon Bragg scattering to measure the intrinsic momentum distribution in a Na condensate.) Figure 6 shows the condensate feature in the Doppler-sensitive part of the two-photon spectrum, plotted relative to the recoil shifted resonance and fit to a Thomas-Fermi density profile.

The atoms giving rise to the feature displayed in Fig. 6, those excited from the condensate by the absorption of two co-propagating photons, pick up enough momentum to be ejected from the trap with a divergence angle of the order of 10^{-3}. They are expected to form a narrow, intense beam of coherent atoms. Although we did not have the instrumentation to detect this beam in our initial experiments, we believe that much interesting physics can be done with this beam in future experiments. Kozuma et al. [22] have used a related process, optically induced Bragg diffraction, to couple sodium atoms out of a Bose-Einstein condensate into coherent wave packets with sharply defined momentum.

If one were to add atoms to a non-interacting

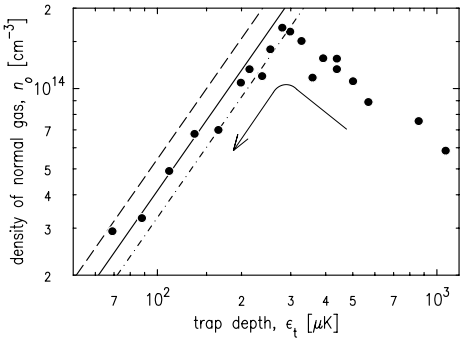

Fig. 7. Density of the normal component of the gas as the trap depth is reduced. The lines (dashed, solid, dot-dashed) indicate the BEC transition line assuming sample temperatures of ($\frac{1}{5}$th, $\frac{1}{6}$th, $\frac{1}{7}$th) the trap depth.

Bose gas held at a fixed temperature the density would increase until it reached a critical value $n_c(T) = 2.612(2\pi m k_B T)^{3/2}/h^3$. If more atoms were added they would condense into the lowest single particle energy eigenstate. The density of the normal component would remain constant. Thus $n_c(T)$, which is virtually unchanged by the presence of a weak interaction, can be regarded as a phase transition line in a plot of the density of the normal component versus temperature. Since the two-photon spectroscopy allows us to determine the densities of the condensate and normal gas separately, we are able to plot our cooling results in exactly this manner.

During cooling by RF evaporation the shape of the magnetic trap is held constant. Although the total number of atoms in the trap decreases, the density of remaining atoms increases since they lose energy and settle deeper into the potential well (see Fig. 7). Once we cool below a certain temperature — determined by the number of atoms in the trap — the density of the normal component decreases along a line consistent with $n_c(T)$.

A plot such as Fig. 7 shows the temperature and the density of the normal component. It does not indicate the size of the condensate under those conditions. That could vary, depending on the number of atoms remaining in the trap. In our experiments the size of the condensate is determined by a balance between the rate at which the atoms leave the

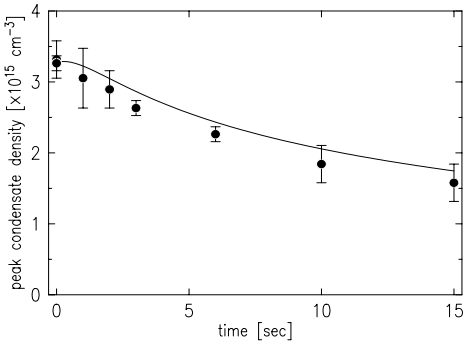

Fig. 8. Time evolution of the peak density in the condensate. The solid curve was generated from a model of the loss mechanisms.

trap due to two-body spin relaxation (primarily in the condensate) and the rate at which the condensate is replenished by atoms from the normal component. As Hijmans et al. have pointed out [23], the weakness of the interaction between the hydrogen atoms limits how far below the transition temperature hydrogen can be taken in an equilibrium situation. The small s-wave scattering length leads to an elastic scattering rate in the thermal cloud well below that in the alkali-metals, thus limiting the evaporative cooling rate. In addition, the weak interaction leads to a high density in the condensate which greatly increases the loss rate. Consequently the condensate fractions that can be obtained in hydrogen are limited to a few percent.

Since the condensate contains only a small fraction of the atoms, the normal gas acts as a large reservoir that continually replenishes the condensate as atoms are lost through dipolar relaxation. This replenishment dramatically increases the apparent lifetime of the condensate. We studied the process by obtaining spectra at various hold times after the end of the forced evaporative cooling cycle. The time evolution of the condensate is displayed in Fig. 8 by plotting the peak condensate density, n_p, as a function of the hold time (here the sample is held without exposure to the probe laser). The peak condensate density decreases by a factor of two (corresponding to a population decrease of $2^{5/2} \simeq 6$) in 15 s. This should be compared to the characteristic condensate decay time due to dipolar relaxation, $\tau_{dip,c} = 7/(2gn_p)$, where $g = 1.2 \times 10^{-15}$ cm^3/s is the dipolar decay rate constant. For $n_p = 2 \times 10^{15}$ cm^{-3}, $\tau_{dip,c} \simeq 1.5$ s. The 15 s lifetime of the condensate thus indicates feeding of the condensate from the thermal cloud.

The number of atoms fed into the condensate roughly matches the number lost during the 15 s shown in Fig. 8. Estimates of the total trap population at $t = 0$ then set an upper limit on the number lost, which scales as $n_p^{7/2}$ [24]. This strong dependence provides a useful consistency check on the determination of the peak condensate density from the observed spectral shift. For example, if n_p were actually a factor of two larger than stated here [20], then the entire normal gas would be expended after the 15 s observation. This is clearly not the case since a large condensate is still present after 15 s.

A simple model [24] of the trapped gas has been used to quantitatively test our understanding of the system. The dynamics are dictated by losses due to dipolar relaxation in the condensate and normal gas, and evaporation from the normal gas. Equilibrium between the normal gas and condensate is assumed. The expected behavior of the condensate is shown by the solid line in Fig. 8. The agreement with experiment indicates a good understanding of the system.

The large reservoir of normal atoms could be useful in the creation of a bright, sustained, CW atom laser. Apparently, in our system 10^9 atoms per second are being condensed out of the normal component. Efficient coupling of these atoms into a coherent beam (instead of losing them from the trap) could have broad applications ranging from fundamental measurements enhanced by entangled quantum states to holographic nanolithography.

The achievement of BEC in hydrogen has attracted wide attention for several reasons. First, it represents the first new Bose-condensed species since the initial alkali experiments. Also, hydrogen condensates are of considerable interest because the interatomic interactions can be calculated to a high degree of accuracy. This may allow preci-

sion tests of not only many-body theories of the condensate but also the theory of ultra-cold collisions. Furthermore, our experiment was the first to exploit high resolution spectroscopy for detection of a condensate. This is noteworthy both for the demonstration of the technique and because the spectroscopy of hydrogen has long been a cornerstone for precision measurements in physics. Great potential exists for further increases in precision using cold, trapped hydrogen.

Acknowledgement

This research is supported by the National Science Foundation and the Office of Naval Research. The Air Force Office of Scientific Research contributed to the early stages. L. W. acknowledges support from Deutsche Forschungsgemeinschaft. D. L. and S. M. are grateful for support from the National Defense Science and Engineering Graduate Fellowship Program.

References

[1] C. E. Hecht, Physica **25**, 1159 (1959)

[2] W. C. Stwalley and L. H. Nosanow, Phys. Rev. Lett. **36**, 910 (1976) and references therein

[3] I. F. Silvera and J. T. M. Walraven, Phys. Rev. Lett. **44**, 164 (1980)

[4] For reviews of the early work on spin-polarized hydrogen see T. J. Greytak and D. Kleppner, in *New Trends in Atomic Physics*, G. Grynberg and R. Stora, eds. (North-Holland, Amsterdam, 1984); I. F. Silvera and J. T. M. Walraven, in *Progress in Low Temperature Physics*, D. F. Brewer, ed. (North-Holland, Amsterdam, 1986), Vol. X; J. T. M. Walraven in *Quantum Dynamics of Simple Systems*, G.-L. Oppo, S. M. Barnett, E. Riis, and M. Wilkinson, eds. (Institute of Physics Publishing, Bristol, 1994)

[5] M. H. Anderson, J. R. Ensher, M. R. Matthews, C. E. Wieman, and E. A. Cornell, Science **269**, 198 (1995)

[6] K. B. Davis, M.-O. Mewes, M. R. Andrews, N. J. van Druten, D. S. Durfee, D. M. Kern, and W. Ketterle, Phys. Rev. Lett. **75**, 3969 (1995)

[7] C. C. Bradley, C. A. Sackett, J. J. Tollett, and R. G. Hulet, Phys. Rev. Lett. **75**, 1687 (1995); C. C. Bradley, C. A. Sackett, and R. G. Hulet, Phys. Rev. Lett. **78**, 985 (1997)

[8] A. I. Safonov, S. A. Vasilyev, I. S. Yasnikov, I. I. Lukashevich, and S. Jaakkola, Phys. Rev. Lett. **81**, 4545 (1998)

[9] T. J. Greytak, in *Bose-Einstein Condensation*, edited by A. Griffin, W. W. Snoke, and S. Stringari (Cambridge University Press, Cambridge, England, 1995). p. 131

[10] H. Hess, Phys. Rev. B **34**, 3476 (1986); T. J. Tommila, Europhys. Lett.**2**, 789 (1986); N. Masuhara, J. M. Doyle, J. C. Sandberg, D. Kleppner, T. J. Greytak, H. F. Hess, and G. P. Kochanski, Phys. Rev. Lett. **61**, 935 (1988)

[11] E. L. Sukov, J. T. M. Walraven, and G. V. Shlyapnikov, Phys. Rev. A **49**, 4778 (1994); Phys. Rev. A **53**, 3403 (1996)

[12] D. E. Pritchard, K. Helmerson, and A. G. Martin, in *Atomic Physics 11*, S. Haroche, J. C. Gay, and G. Grynberg eds. (World Scientific, Singapore, 1989), p. 179

[13] W. Petrich, M. H. Anderson, J. R. Ensher, and E. A. Cornell, Phys. Rev. Lett. **74**, 3352 (1995); K. B. Davis, M.-O. Mewes, M. A. Joffe, M. R. Andrews, and W. Ketterle, Phys. Rev. Lett. **74**, 5202 (1995)

[14] J. M. Doyle, J. C. Sandberg, N. Masuhara, I. A. Yu, D. Kleppner, and T. J. Greytak, J. Opt. Soc. Am. B **6**, 2244 (1989)

[15] C. L. Cesar, D. G. Fried, T. C. Killian, A. D. Polcyn, J. C. Sandberg, I. A. Yu, T. J. Greytak, D. Kleppner, and J. M. Doyle, Phys. Rev. Lett. **77**, 255 (1996)

[16] M. J. Jamieson, A. Dalgarno, and J. M. Doyle, Mol. Phys., **87**, 817 (1996)

[17] T. C. Killian, D. G. Fried, L. Willmann, D. Landhuis, S. C. Moss, T. J. Greytak, and D. Kleppner, Phys. Rev. Lett. **81**, 3807 (1998)

[18] D. G. Fried, T. C. Killian, L. Willmann, D. Landhuis, S. C. Moss, D. Kleppner, and T. J. Greytak, Phys. Rev. Lett. **81**, 3811 (1998)

[19] M. J. Jamieson, A. Dalgarno, and M. Kimura, Phys. Rev. A **51**, 2626 (1995)

[20] In the spectroscopic determination of the condensate density we have used the same constant of proportionality χ between the frequency shift and the density that we found for the normal gas. For excitation out of a Bose condensate the absence of exchange effects should reduce χ by a factor of 2. If this were the case the maximum density in the condensate would be twice as high and the condensate fraction calculated from the Thomas-Fermi analysis would be 25%, inconsistent with the value obtained from the relative spectral weights. We do not as yet understand the origin of this discrepancy.

[21] J. Stenger, S. Inouye, A. P. Chikkatur, D. M. Stamper-Kurn, D. E. Pritchard, and W. Ketterle, Phys. Rev. Lett. **82**, 4569 (1999)

[22] M. Kozuma, L. Deng, E. W. Hagley, J. Wen, R. Lutwak, K. Helmerson, S. L. Rolston, and W. D. Phillips, Phys. Rev. Lett. **82**, 871 (1999)

[23] T. W. Hijmans, Y. Kagan, G. V. Shlyapnikov, and J. T. M. Walraven, Phys. Rev. B **48**, 12886 (1993)

[24] D. G. Fried, Ph.D. thesis, Massachusetts Institute of Technology, 1999